



5-2007

A Simulation Model for Predicting Surface Tension in Condensate Films

Allison Dawn Lewis
University of Tennessee - Knoxville

Follow this and additional works at: https://trace.tennessee.edu/utk_gradthes



Part of the [Biomedical Engineering and Bioengineering Commons](#)

Recommended Citation

Lewis, Allison Dawn, "A Simulation Model for Predicting Surface Tension in Condensate Films. " Master's Thesis, University of Tennessee, 2007.
https://trace.tennessee.edu/utk_gradthes/299

This Thesis is brought to you for free and open access by the Graduate School at TRACE: Tennessee Research and Creative Exchange. It has been accepted for inclusion in Masters Theses by an authorized administrator of TRACE: Tennessee Research and Creative Exchange. For more information, please contact trace@utk.edu.

To the Graduate Council:

I am submitting herewith a thesis written by Allison Dawn Lewis entitled "A Simulation Model for Predicting Surface Tension in Condensate Films." I have examined the final electronic copy of this thesis for form and content and recommend that it be accepted in partial fulfillment of the requirements for the degree of Master of Science, with a major in Biomedical Engineering.

Don Dareing, Major Professor

We have read this thesis and recommend its acceptance:

Jack Wasserman, Richard Jendrucko

Accepted for the Council:

Carolyn R. Hodges

Vice Provost and Dean of the Graduate School

(Original signatures are on file with official student records.)

To the Graduate Council:

I am submitting herewith a thesis written by Allison Dawn Lewis entitled “A Simulation Model for Predicting Surface Tension in Condensate Films.” I have examined the final electronic copy of the thesis for form and content and recommend that it be accepted in partial fulfillment of the requirements for the degree of Master of Science, with a major in Biomedical Engineering.

Don Dareing
Don Dareing, Major Professor

We have read this thesis
and recommend its acceptance:

Jack Wasserman

Richard Jendrucko

Acceptance for the Council:

Carolyn R. Hodges
Vice Provost and
Dean of the Graduate School

(Original signatures are on file with official student records)

A Simulation Model for Predicting Surface Tension in Condensate Films

A Thesis
Presented for the
Master of Science
Degree
The University of Tennessee, Knoxville

Allison Dawn Lewis
May 2007

Copyright ©2007 by Allison Dawn Lewis
All rights reserved

Acknowledgements

I wish to thank all of those who helped me complete my Masters of Science degree in Biomedical Engineering. I would like to thank Dr. Dareing for all his support and encouragement during the course of this study. I would also like to thank Dr. Jendrucko and Dr. Wasserman for being a part of my thesis committee. Lastly I would like to express my appreciation to my family and friends who continually encouraged me and made this work possible.

Abstract

The thesis presents a mathematical model for predicting surface tension in condensate films. The approach taken to this study is different from how surface tension is normally approached. Surface tension is primarily determined through laboratory measurements. This work shows how it can be determined mathematically based on the formulation of bonding energy between atoms as described by the Lennard-Jones potential.

The results are used to predict the surface tension of a selected group of elements and molecules. Predictions from the model compare favorably with the documented surface tension values of the selected elements. However, the model does deviate somewhat from the documented surface tension values for the larger molecules. This model should be useful in formulating the response of various nano and micro systems to capillary action.

Table of Contents

I. Introduction.....	1
II. Objective of Study.....	11
III. Capillary Forces.....	12
IV. Mathematical Methodology.....	18
Configuration 1- atomic ring with no pressure.....	19
Configuration 2- atomic ring with internal pressure.....	21
Configuration 3- atomic sphere with no pressure.....	25
Configuration 4- atomic sphere with internal pressure.....	27
V. Discussion of Results.....	29
Configuration 1- atomic ring with no pressure.....	31
Configuration 2- atomic ring with internal pressure.....	31
Configuration 3- atomic sphere with no pressure.....	32
Configuration 4- atomic sphere with internal pressure...	33
VI. Comparison with documented surface tension.....	33
VII. Conclusion.....	40
Bibliography.....	41
Appendix.....	45
Vita.....	51

List of Figures

1. Potential Energy between two atoms: $A=1.0E-4$ nN-nm nm ⁶ & $B=1.0E-7$ nN-nm nm ¹²	5
2. Resultant Force between two atoms: $A=1.0E-4$ nN-nm nm ⁶ & $B=1.0E-7$ nN-nm nm ¹²	7
3. Capillary geometry to define r_e and r_{max}	9
4. Types of capillary forces [12].....	13
5. Free Body Diagram of spherical bubble.....	15
6. Basic Lennard-Jones Diagram.....	18
7. Atomic Ring with no internal pressure	20
8a. Atomic Collar	22
8b. Atomic Collar.....	22
9. Atomic Ring Diagram with pressure diagram.....	24
10a. Basic nesting pattern assumed for analysis.....	26
10b. Basic nesting pattern along great circle.....	26
11. Atomic Sphere with internal pressure along great circle.....	28
12. Depiction for pressure determination.....	35

List of Tables

1. Lennard Jones Values.....	29
2. Determination of Surface Tension Hg.....	36
3. Surface Tension Comparison of basic elements.....	37
4. Surface Tension Comparison of Molecules.....	39
A.1. Determination of Surface Tension CCl ₄	46
A.2. Determination of Surface Tension H ₂ O.....	47
A.3. Determination of Surface Tension Ne.....	47
A.4. Determination of Surface Tension Ar.....	48
A.5. Determination of Surface Tension He.....	48
A.6. Determination of Surface Tension Kr.....	49
A.7. Determination of Surface Tension Xe.....	49
A.8. Determination of Surface Tension CO ₂	50

List of Symbols

A, B	- Dimensional Lennard Jones constant
e	-radial displacement of an element
F	-force equation
F_{\max}	-maximum Force
ℓ	-length of atomic collar
n	-number of atoms
p	-pressure
P_{cr}	- critical pressure force
r	-separation distance between atoms
r_e	-equilibrium separation
r_{\max}	- max separation
R	-distance from the center of ring and sphere to the outside
t	-thickness of wall
$V = V(e)$	-minimal potential energy principle
$w(r)$	-potential energy
γ	-surface tension
σ_1	-stress in wall of spherical pressure vessel
σ	-non dimensional Lennard Jones constants

- ε -non dimensional Lennard Jones constants
- θ -angle between atoms
- Ω -potential energy of external force, P

I. Introduction:

Surface interfaces occur everywhere, with the new technologies being developed especially in nanotechnology there is an important need to understand surface properties [1]. Surface tension, one of these surface properties, is defined as an effect that causes a liquid to behave like an elastic sheet [2]. The phenomenon scientists know as surface tension is caused by the cohesive forces between liquid molecules. Cohesive forces are forces that occur between like molecules. Surface tension is one of the most important concepts when dealing with interfaces; the effects that arise from it play a role in the behavior of systems [1]. It is measured in force per unit length, generally in mN/m, milliNewtons per meter. Surface tension is important because of its widespread applications. It is evident in our everyday lives with the beading of water droplets, lubricating surfaces, the material of a tent, along with other daily occurrences. Applications extend beyond the everyday and are seen in the medical field, thermodynamics, chemistry, and other scientific areas [3].

There are several documented experimental methods for measuring surface tension:

1. Tensiometry: measurement of surface and interfacial tension by a tensiometer. Tests are “based on force measurement of the interaction of a probe with the surface of interface of two fluids” [4]. Mathematical interpretation is based on the shape of the probe.
2. DuNoüy Ring method: one of the probes used in tensiometry; interaction between a platinum ring with the surface.
Traditional method to measure surface tension.
3. Wilhelmy Plate method: other probe used in tensiometry; interaction between platinum plate with surface. Universal method especially to check surface tension over long duration intervals.
4. Spinning Drop method: ideal for measuring low interfacial tensions.
5. Pendant Drop Shape Analysis: useful for high temperatures and pressures. Bubbles geometry is analyzed.
6. Jaeger’s method (bubble pressure): determine surface tension at short surface ages, maximum pressure measured.

7. Drop Volume method: determine surface tension as a function of interface age [4,5].

Since surface tension plays an important part in everyday life, formulating a model to predict these values is extremely useful as an analytical tool. The motivation for this model is to formulate surface tension to put us in a better position to integrate capillary phenomena, giving the purpose that the model allows surface tension to be analytically determined. To do this there has to be knowledge of the fundamental engineering mechanics that are based on the use of atomic bonding energy, as defined by the Lennard Jones potential. With our present knowledge predicting surface tension analytically is something that does not exist except in laboratory experiments.

The ability to predict surface tension is useful in the advancement of technology. With advancements in technology, the mechanics of surface tension can be interfaced with nano and micro structures. Nanotechnology is an emerging leader in the field of science and engineering research. It is defined by early promoter Albert Franks as “that area of science and technology where dimensions and tolerances in the range of 0.1 nm to 100 nm play a critical role” [6]. With the

invention of the Scanning Tunneling Microscope (STM) by Binnig & Rohrer in the early 1980s, the ability for researchers to look at the applications of mechanics on the micro and nano levels becomes more than a thought; it becomes a reality. The continued development of nanotechnology has applications in the real world with breakthroughs in areas such as material, manufacturing, medicine, energy, biotechnology, and national security [7]. It is important to know the scale being examined when working on the nano level. It is generally agreed that:

1. nano range is atomic to 100nm
2. the micro scale range is 100 nm to 500 μ m
3. the macro scale range is 500 μ m and above

It is also important to note that 1 angstrom=0.1nm.

Bonding mechanisms of atoms directly affect the force-deformation relationships. Structural components and the behavior of nano structures are analyzed by the properties of these bonds.

Chemically bonded atoms are formed from atoms sharing electrons, making these strong bonds. Chemical bonds hold the atoms within a molecule together forming what is commonly referred to as a slightly rigid structural component.

Lennard-Jones potential is used as a description of the interaction between chemically bonded atoms [8]. The Lennard-Jones potential formula is a mathematical approximation of how atoms in an attached film are attracted and repulsed.

$$\omega(r) = \frac{-A}{r^6} + \frac{B}{r^{12}} \quad (1)$$

$$F = \frac{dw}{dr} = \frac{6A}{r^7} - \frac{12B}{r^{13}} \quad (2)$$

A and B are known as the Lennard-Jones constants, with a specific value for each element and molecule. The values are determined by the bonding and non-bonding mechanisms at the surface interfaces. These two equations are represented in Figures 1 and 2[2].

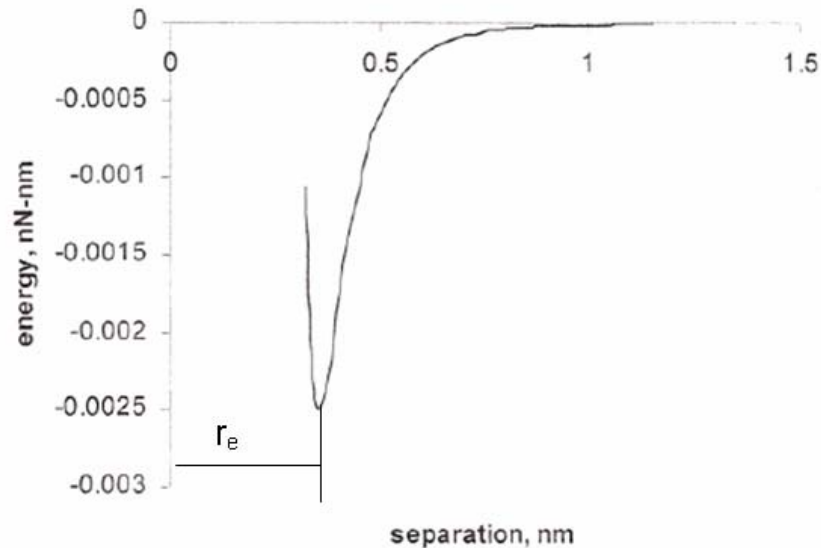


Figure 1: Potential Energy between two atoms :A=1.0E-4nN-nm nm⁶ & B=1.0E-7 nNnm nm¹²

The results of a representative bonding model is shown in Figures 1 and 2. In Figure 1 the energy of the film decreases as the equilibrium separation increases. When the energy of the film reaches its equilibrium position, the energy will reach a trough. Similar to Figure 1, in Figure 2 there is a representation of the simplest behavior of the force with respect to separation distance. In Figure 2 the force increases with the increase of separation, and at r_{\max} the force reaches a maximum. With regard to capillary films, the “bubble” will burst when r is greater than r_{\max} .

Using distance between two atoms to model the potential energy makes the Lennard-Jones potential an empirical relationship. The Lennard-Jones potential for w has two forms that are represented by equations 3 and 5[9, 10]. These two sets of constants σ , ε , A , and B are related to each other through the equations 4, 6, and 7.

$$w(r) = 4\varepsilon \left[\left[\frac{\sigma}{r} \right]^{12} - \left[\frac{\sigma}{r} \right]^6 \right] \quad (3)$$

$$\sigma = \left(\frac{B}{A} \right)^{1/6} \quad \varepsilon = \frac{A^2}{4B} \quad (4)$$

$$w(r) = \frac{B}{r^{12}} - \frac{A}{r^6} \quad (5)$$

$$A = 4\varepsilon\sigma^6 \text{ J m}^6 \quad (6)$$

$$B = 4\varepsilon\sigma^{12} \text{ J m}^{12} \quad (7)$$

The constants of sigma (σ) and epsilon (ϵ) are based on the materials.

The non- dimensional form of the Lennard-Jones potential uses the sigma and epsilon to determine potential energy. The dimensional form examined during this study uses the constants of A and B, equations 6 and 7. The units for A are [J m^6] and for B are [J m^{12}]. However, since we are dealing with the nano scale, the units will be [$(\text{nN nm}) \text{nm}^6$] and [$(\text{nN nm}) \text{nm}^{12}$] respectively [9, 10].

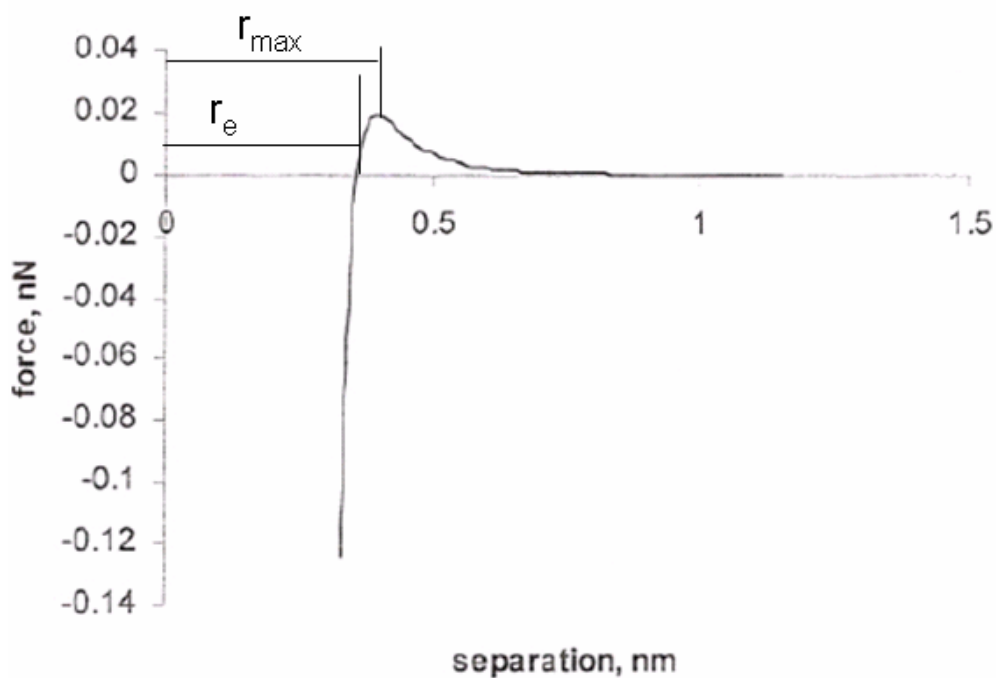


Figure 2: Resultant Force between two atoms: $A=1.0E-4\text{nN-nm nm}^6$ & $B=1.0E-7 \text{nN-nm nm}^{12}$

The geometry shown in Figure 3 is fundamental to this study. The atomic arrangement coupled with the Lennard-Jones potential, leads to the definition of equilibrium separation, r_e , and maximum separation, r_{\max} . To determine equilibrium separation, the derivative of the Lennard-Jones energy equation, equation 1 is set equal to zero and then solved for r . Under this condition $r=r_e$. The same process occurs for the determination of r_{\max} . To define the equation for r_{\max} , the derivative of the Lennard-Jones force equation, equation 2 is set equal to zero and then solved for r . Under this condition $r=r_{\max}$. Equations 8 through 13 show how r_e and r_{\max} are developed.

$$\frac{dw}{dr} = 0 \quad (8)$$

$$\text{Solve for } r = r_e \quad (9)$$

$$r_e = \frac{13B}{6A} \quad (10)$$

$$\frac{dF}{dr} = 0 \quad (11)$$

$$\text{Solve for } r = r_{\max} \quad (12)$$

$$r_{\max} = \left[\frac{12 \times 13 \times B}{42A} \right]^{1/6} \quad (13)$$

This study focuses on the development of a mathematical model to predict surface tension using the Lennard-Jones potential. Specifically, the mathematical model developed will provide an engineering tool for interfacing surface tension mechanics with nano and micro systems. The following sections explain the model simulations of surface tension and demonstrate how the model is used to relate pressure to capillary geometries. Of a particular interest is the relationship between the predicted surface tension and bubble pressure. This relationship provides the check on our analytically determined surface tension.

There will also be a development of the mechanics of surface tension for the following four configurations:

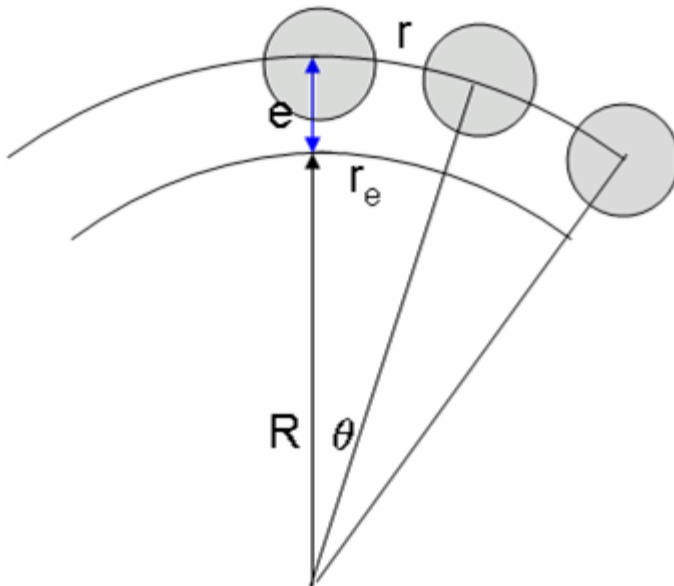


Figure 3: Capillary geometry to define r_e and r_{\max}

1. Atomic ring with no pressure
2. Atomic ring with internal pressure
3. Atomic sphere with no pressure
4. Atomic sphere with internal pressure

The prediction of surface tension is derived from the Lennard Jones potential, capillary geometries, and the mathematical methodology. The final portion of this study focuses on the comparison of the calculated surface tension to what is documented in literature, based on previous experiments.

II. Objective of Study

Currently surface tension is determined experimentally in the laboratory. The objective of this research is to develop a simulation model that can be used to mathematically predict surface tension. This model should be a useful engineering tool for predicting the deflections in micro and nano structures caused by capillary forces. Application of the simulation model developed in this study, on various elements of documented surface tensions, shows that the method presented in this work gives predicted surface tensions that are in agreement with the documented data.

III. Capillary Forces

A function of separation distance, commonly encountered in nature is capillary forces. These forces are the results of the surface energy and tension on the surface of liquids [2]. The spontaneous condensation of liquids from surrounding vapor leads to the formation of a liquid bridge. The relationship is developed on either the basis of total energy of solid surfaces interacting through liquid and ambient vapor or by direct calculation of the force [11]. These forces are important to the understanding of micro mechanisms because of the possible presence of humidity and condensation between the engaged surfaces.

Peter Kralchevsky and Nikolai Denkov in their article “Capillary forces and structuring in layer of colloid particles” investigate the advances in science involving capillary forces. In general “capillary forces are interactions between particles mediated by fluid interfaces” [12]. The interest in these types of forces has grown due to the recognition of their importance in the self-assembly of macro and microscopic particles and molecules. In Figure 4 there is a representation of the different types of capillary forces that are found occurring in nature [12].

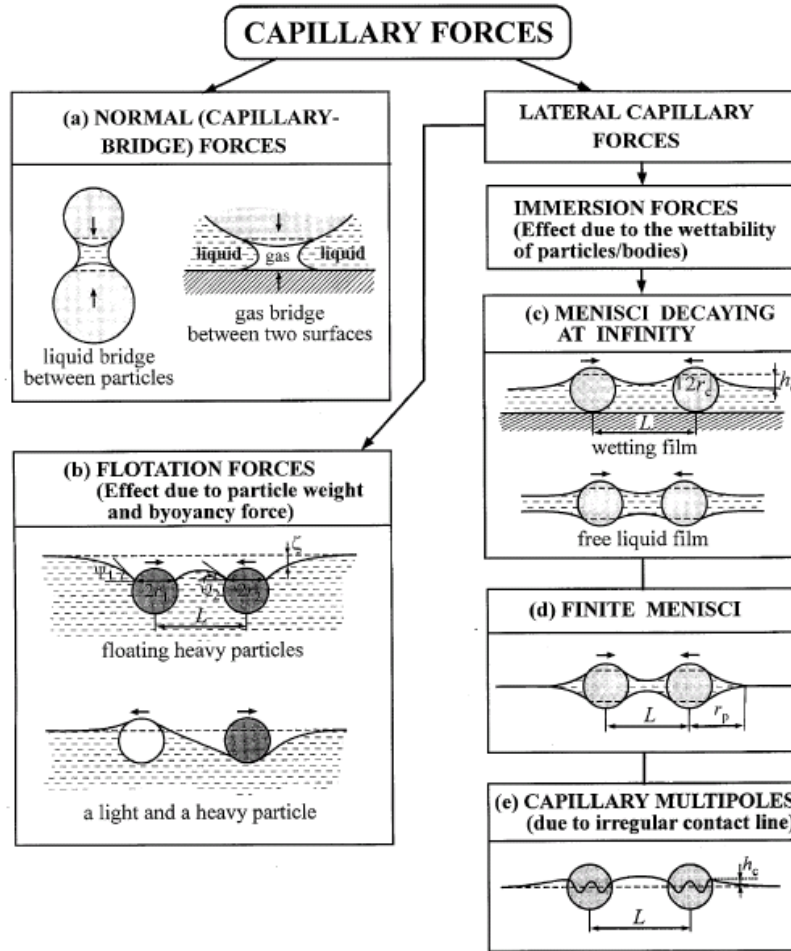


Figure 4: Types of Capillary Forces [12]

At any point the local capillary force on a fiber-liquid-vapor triple line can have a magnitude equal to the surface tension and the direction perpendicular to the triple tangent vector \vec{dl} . Local capillary force vectors must satisfy four constraints:

1. Is at an angle, the contact angle, to the fiber tangent surface so that $\vec{F} \cdot n = \gamma \sin \theta$
2. Where n is the outward fiber surface normal of unit length
3. Is perpendicular to edge tangent vector \vec{dl} so that $\vec{F} \cdot \vec{dl} = 0$, the magnitude $|\vec{F}|$ is γ ; the surface tension
4. The edge integral makes a clockwise loop around the fiber, the solder droplet will always be on the left, so that $\theta < 90^\circ, n \times \vec{F} \cdot \vec{dl} > 0 (< 0 \text{ for } \theta > 90^\circ)$ [13]

To better understand or visualize the free surface energy the analogy of elastic membranes is often used. Surface tension is a physical property of liquids; if a liquid is entrapped by a “membrane,” it achieves a pressure and shape that is in equilibrium with the surface tension.

While the membrane analogy helps in understanding, there is a basic difference between elastic membranes and surface tension. With surface

tension the film tension remains constant, and the pressure falls off as the radius of the bubble increases. However, with the membrane analogy, the tension increases as radius increases, and the pressure remains constant. Equation 14 is a representation of internal pressure, and equation 15 is a spherical pressure vessel as represented in Figure 5. These equations will be used in the development of the mathematical simulations that involve internal pressure to be able to compare surface tension [2]. Presently surface tension for liquids and gases are determined experimentally.

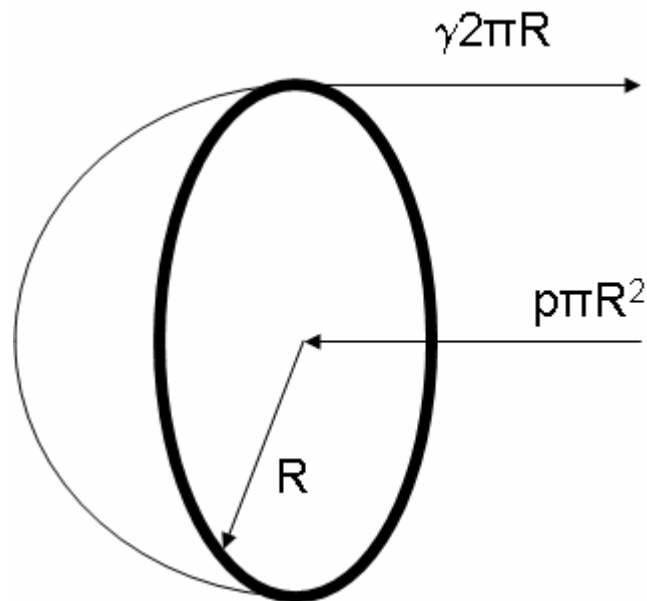


Figure 5: Free Body Diagram of spherical bubble

$$p = \frac{2\gamma}{R} \quad (14)$$

$$p = \frac{2\sigma_1 t}{r} \quad (15)$$

Within bubbles there are three different states of matter: gas, liquid, and solid. For the purpose of this study it is important to talk about the states of gases and liquids within a bubble to develop a better understanding of how capillary forces and surface tension play a role.

Examining at the properties of gases, it is known that gases:

1. Assume the shape and volume of the container
2. Have compressibility; maximum space between particles
3. Flow easily

The same type of information is examined for the liquid state as well.

Liquids:

1. Assume the shape of the container which they occupy
2. Are not easily compressible; little free space between the particles
3. Flow easily[14]

For a gas within a bubble the knowledge of a gas's property allows us to conclude that the radius of the film will be much greater than that of the

equilibrium radius throughout the entire bubble. However, the same cannot be said for a liquid within a bubble. Atoms on the surface of a liquid have no neighboring atoms above them; consequently, they are attracted more strongly to the atoms below them. This attraction forms a “film” on the surface, which makes objects more difficult to move through that surface than when submerged [5]. This knowledge allows the relationship between the radius, the equilibrium radius and r_{\max} to be determined. In the case of a liquid within a bubble on the surface where the film is formed, the radius is less than that of the r_{\max} . But this is only true for the surface of the bubble; when examining at the interior of the bubble this cannot be concluded. Within the interior of a bubble the molecules are free to move within the space so the radius is greater than that of the r_{\max} . It is also concluded from the properties of a liquid that within liquids a static force can not be supported, but the strength of the film is based on the bonding of the atoms on the surface.

IV. Mathematical Methodology

This section develops the mathematical formulation of the four configurations being studied.

1. Atomic ring with no pressure
2. Atomic ring with internal pressure
3. Atomic sphere with no pressure
4. Atomic sphere with internal pressure

These configurations are chosen for their relevance to the Lennard-Jones potential.

To comprehend the response of the Lennard-Jones potential, it is critical to start with a basic model and develop the basic understandings of how it behaves. Figure 6, a representation of the basic setup of the simplest model, shows two atoms connected at a separation distance of r .

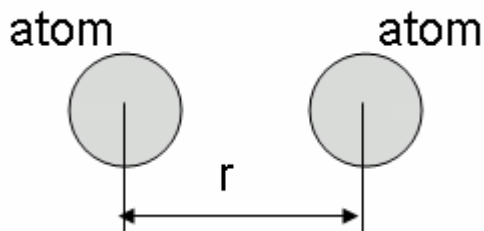


Figure 6: Basic Lennard-Jones Model

Both energy and force reach an equilibrium separation (r_e), which occurs when the atoms in the film reach an equilibrium state. Values that occur before the r_e is reached are the forces that can be withstood without the film (bubble) bursting. The values of energy and force that are produced after equilibrium separation occur after the film has burst.

Configuration1- atomic ring with no pressure

From the two atom model, a mathematical model is developed as a representation of an atomic ring. The atoms are separated by a separation distance r , an angle of theta (θ), a radius R from the center of the ring, and no internal pressure. In figure 7 a diagram of the atomic ring gives an idea of how the model is able to change within the Lennard-Jones energy and force equations.

The equation developed is a change in separation distance r between the atoms.

$$r = 2R \sin(\theta / 2) \quad (16)$$

The development of the equation of radius R is derived from the new equation for separation distance. In equations 1 and 2 separation distance is replaced with equation 16 producing the following equations for energy and force.

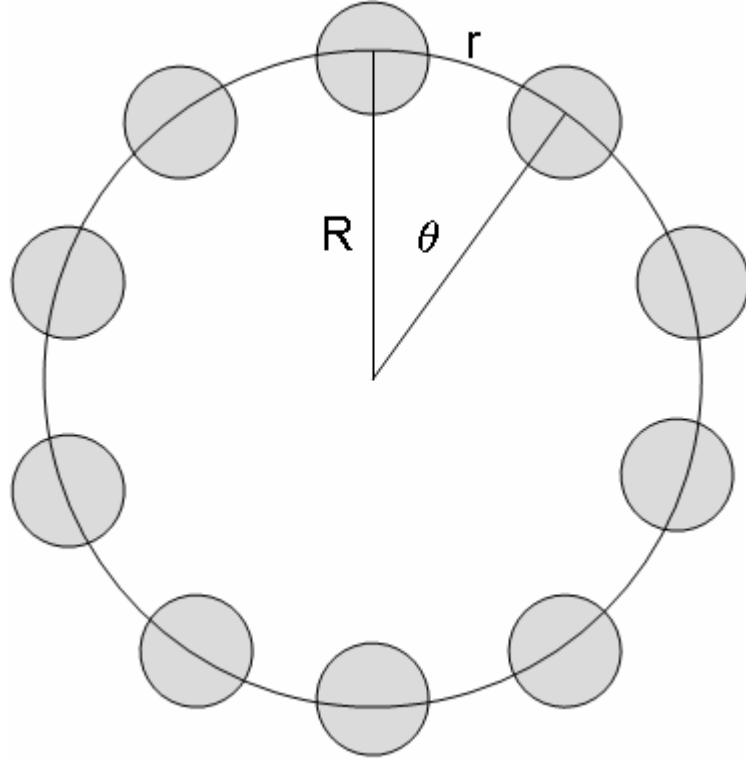


Figure 7: Atomic Ring with no internal pressure.

$$w(R) = \frac{-A}{(2R \sin(\theta/2))^6} + \frac{B}{(2R \sin(\theta/2))^{12}} \quad (17)$$

$$F(R) = \frac{6A}{(2R \sin(\theta/2))^7} - \frac{12B}{(2R \sin(\theta/2))^{13}} \quad (18)$$

R is determined by setting $\frac{dw}{dR} = 0$ allowing:

$$\frac{6A}{(2 \sin(\theta/2))^6 (R)^7} = \frac{12B}{(2 \sin(\theta/2))^{12} (R)^{13}} \quad (19)$$

From this equation R is developed such that

$$R = \left[\frac{12B}{6A(2 \sin(\theta/2))^6} \right]^{1/6} \quad (20)$$

With R being established, the equilibrium separation distance between the atoms is also determined. From the determination of radius, theta and separation, the values for energy and force with the atomic ring are produced. Figures 8a and 8b are an atomic collar representation of the atomic ring. From the atomic collar the following equations are determined:

$$p\ell 2r = 2\gamma\ell \quad (21)$$

$$p = \frac{\gamma}{r} \quad (22)$$

Configuration 2- atomic ring with internal pressure

The atomic ring with pressure model is a slight variation from the no pressure model of configuration 1. In the second configuration, an internal pressure force is placed within the atomic ring causing a force that pushes outwards. Figure 9 is a section view of the atomic ring with an internal pressure that causes the atoms to move out a distance e from the radius determined in configuration 1. The addition of an internal force has changed equations 1, 2, and the distance r between the atoms. The distance equation 17 becomes:

$$r = 2(R + e) \sin(\theta / 2) \quad (23)$$

with R and θ from configuration 1.

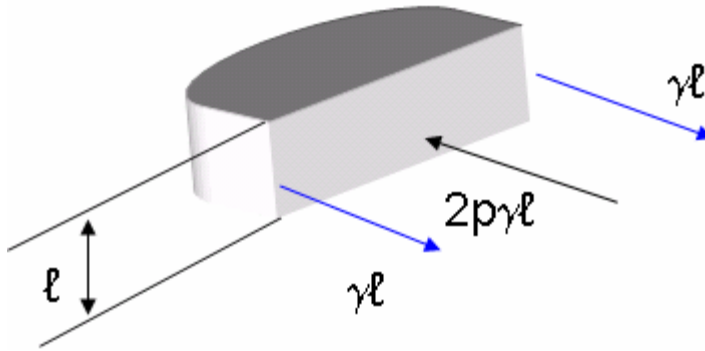


Figure 8a: Atomic Collar

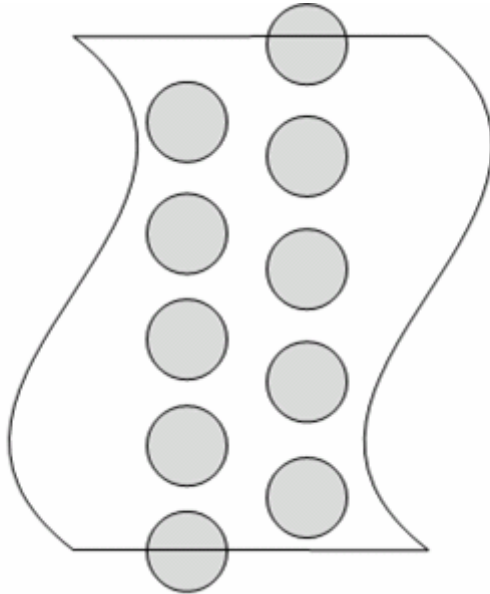


Figure 8b: Atomic Collar

The minimum potential energy principle is a fundamental concept in several scientific areas, such as physics, chemistry, and thermodynamics. In the second configuration the addition of internal pressure is utilized; to add the term Ω to the model, the minimum potential energy principle must be used. Equation 24a is the basic equation used by this principle; the total potential energy is the sum of bond energy and the potential energy. For the purpose of this study the U in equation 24a is replaced with the w coming from the Lennard Jones potential equations [15].

$$V = U + \Omega \quad (24a)$$

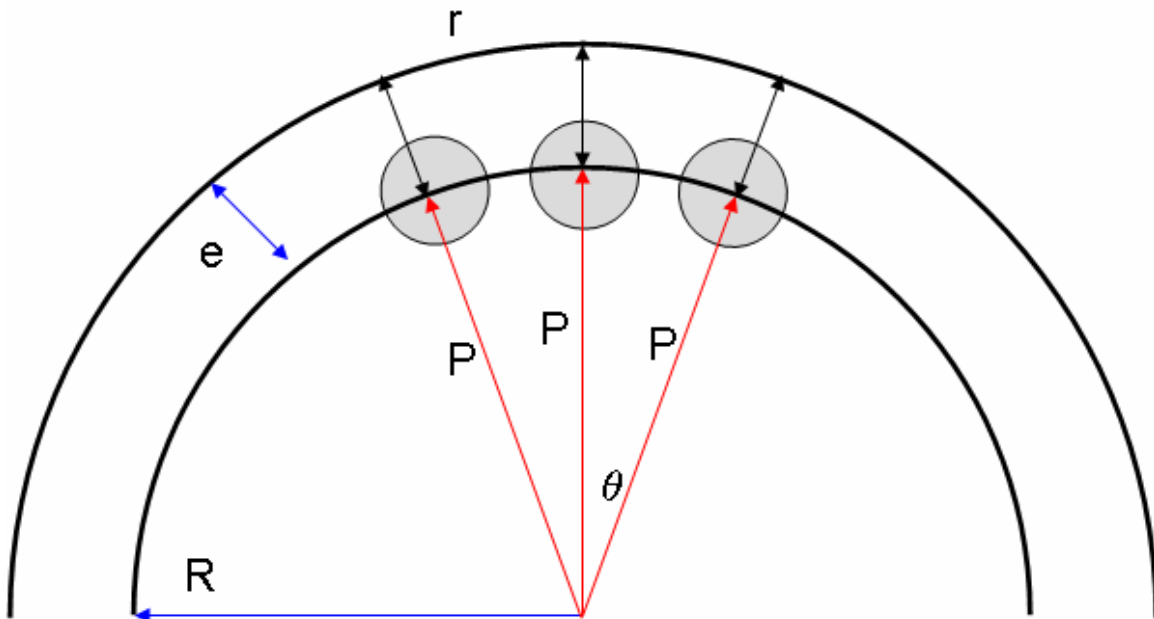


Figure 9: Atomic Ring Diagram with pressure.

$$V = w + \Omega \quad (24b)$$

$$V = V(e) \quad (25)$$

$$\frac{dV}{de} = 0 \quad \text{solve for } e \quad (26)$$

In addition to the added term in the distance equation there is also the addition of energy Ω with P being the force pressing outwards.

$$\Omega = -Pe \quad (27)$$

Producing energy and force equations:

$$w(e) = \frac{-A}{(2(R+e)\sin(\theta/2))^6} + \frac{B}{(2(R+e)\sin(\theta/2))^{12}} - Pe \quad (28)$$

$$F(e) = \frac{6A}{(2(R+e)\sin(\theta/2))^7} - \frac{12B}{(2(R+e)\sin(\theta/2))^{13}} - P \quad (29)$$

From the equation $\frac{dw}{de} = 0$, the equation for e is determinable.

$$e = \left[\frac{6A(2\sin(\theta/2))^6 - 12B}{P(2\sin(\theta/2))^{12}} \right]^{1/7} - R \quad (30)$$

The determination of e produces the separation distance between the atoms in the atomic ring. Configuration 2 force and energy values are compared to those of configuration 1 to see how pressure affects the equilibrium state of the atomic ring.

Configuration 3- atomic sphere with no pressure

The third configuration designed for the study involves a film in the shape of a sphere. Mathematically a sphere is known as a perfectly symmetrical, three dimensional geometric object [16]. Figure 10a gives a depiction of the basic nesting pattern of atoms being assumed in the study. The hexagonal pattern is essential to the model. Figure 10b is a section view of the hexagonal pattern along the great circle.

To find the equation of theta a sphere must be divided into regions. A sphere is split into two hemispheres and then divided into four regions, each of which has two sides that are segments of a great circle [17, 18].

$$r = R(\theta) \quad (31)$$

A great circle has the same center and radius as the sphere. Antipodal points occur on the surface of the sphere and are located diametrically opposite to another point so that when a line is drawn from one to the other the line will pass through the center of the sphere.

The segments of the great circle are called lunes or biangles. A lune is the intersection of 2 hemispheres. In a lune two things must be true: the vertices are antipodal points, and the two angles are equal [18].

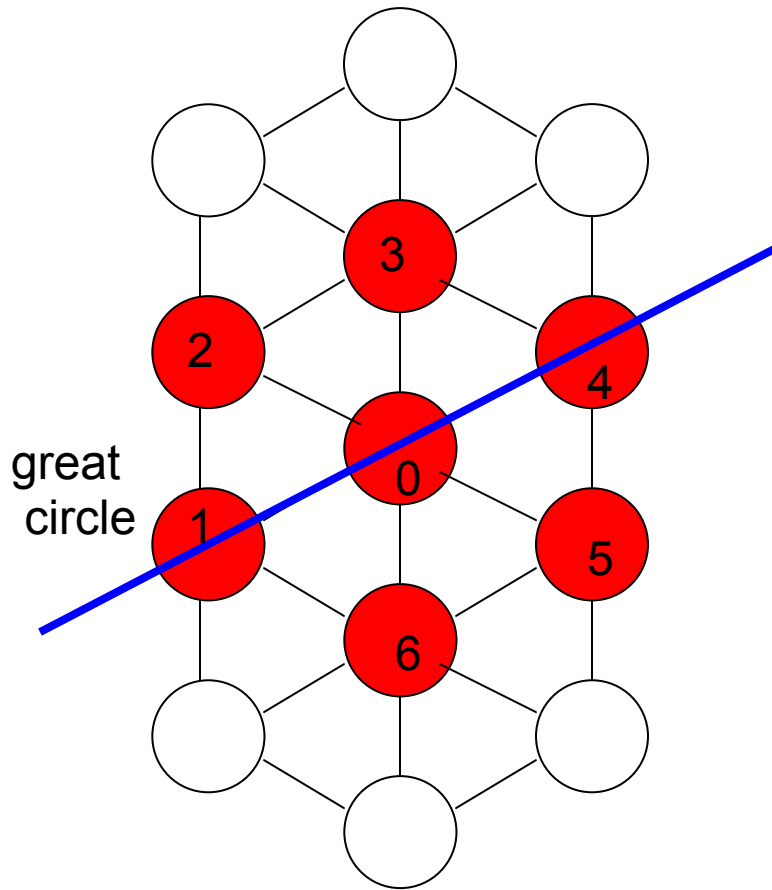


Figure 10a: Basic nesting pattern assumed for analysis

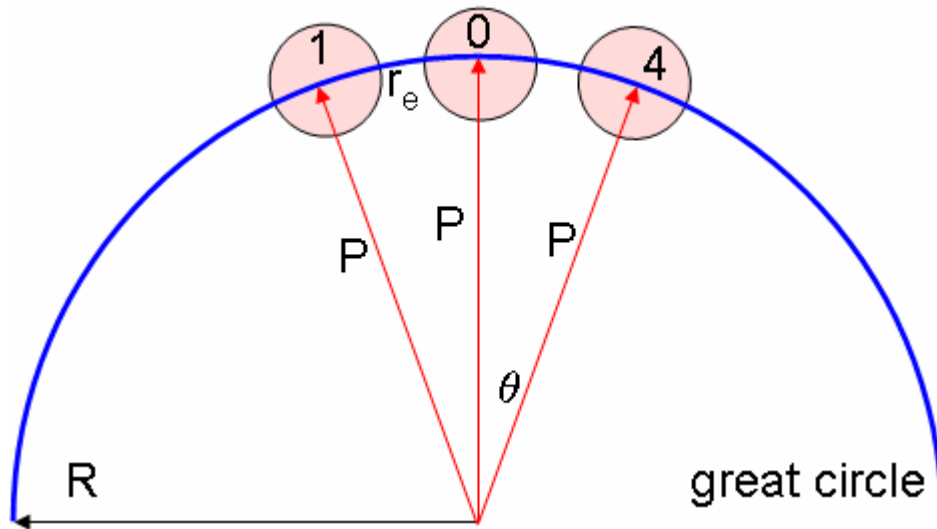


Figure 10b: Basic nesting pattern along great circle

To determine the radius R, the value of r is replaced producing equations 34 and 35.

$$w(R) = \frac{-A}{(R(\theta))^6} + \frac{B}{(R(\theta))^{12}} \quad (32)$$

$$F(R) = \frac{6A}{(R(\theta))^7} - \frac{12B}{(R(\theta))^{13}} \quad (33)$$

From the equation $\frac{dw}{dR} = 0$, the equation for R is determined.

$$R = \left[\frac{12B}{6A\theta^6} \right]^{1/6} \quad (34)$$

Configuration 4-atomic sphere with internal pressure

The final configuration in this study is a variation of the third configuration. Figure 11 demonstrates the addition of pressure to a sphere causing the atoms in the sphere to move outwards a distance of e from the radius R that comes from configuration 3. There is an addition of a pressure term to the energy and force equations. The geometry of the sphere from Figure 11 produces the equation for separation distance:

$$r = (R + e)(\theta) \quad (35)$$

Equation 37 replaces the r in equations 1 and 2 producing equations 38 and 39.

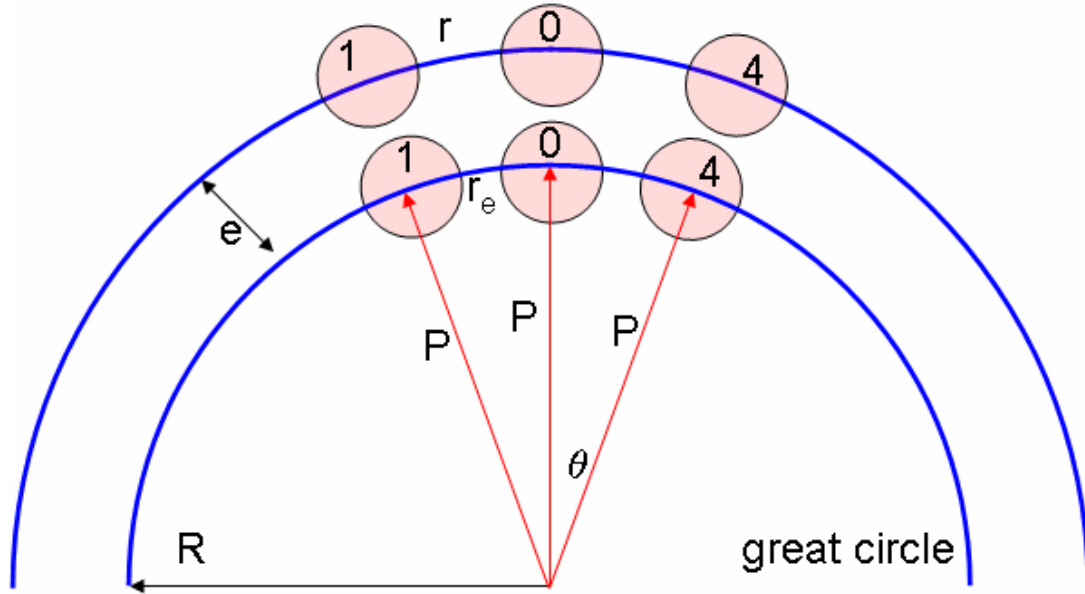


Figure 11: Atomic Sphere with internal pressure along great circle

$$w(e) = \frac{-A}{((R+e)(\theta))^6} + \frac{B}{((R+e)(\theta))^{12}} - Pe \quad (36)$$

$$F(e) = \frac{6A}{((R+e)(\theta))^7} - \frac{12B}{((R+e)(\theta))^{13}} - P \quad (37)$$

From setting $\frac{dw}{de} = 0$, the equation for e is determined. The e leads to the production of the separation distance between atoms.

$$e = \frac{R^2\theta - Rr_e}{r_e - R\theta} \quad (38)$$

The values of energy and force, when modeled against separation distance, demonstrate how the pressure affects the equilibrium positioning determined in configuration 3.

V. Discussion of Results

The development of the mathematical simulations allows for the discussion and comparison of the Lennard-Jones potential energy and force equations. To understand the results that occur, the basic model must be examined. The basic two atom model shows that both the energy and force are directly connected to equilibrium separation. This connection can be seen through the Lennard-Jones potential equations and the results of the basic model, which are represented in Table 1.

For simplicity, the configurations discussed have Lennard-Jones constants of A and B equaling:

$$A=1.0E-4 \text{ nN-nm nm}^6$$

Table 1: Lennard Jones Values

Element	σ (m)	ϵ (J)	A Lennard Jones constant (J m^6)	B Lennard Jones constant (J m^{12})	A Lennard Jones constant (nN-nm nm^6)	B Lennard Jones constant (nN-nm nm^{12})
in general [22]	3.16E-10	2.50E-21	1.00E-76	1.00E-133	1.00E-04	1.00E-07
CCl ₄ [19]	5.88E-10	4.51E-21	7.46E-76	3.08E-131	7.46E-04	3.08E-05
Hg [19]	2.9E-10	1.174E-20	2.79E-77	1.66E-134	2.79E-05	1.66E-08
H ₂ O [8]	3.17E-10	1.08E-21	4.34E-78	4.36E-135	4.34E-6	4.36E-9
Ne [19]	2.75E-10	4.92E-22	8.51E-79	3.68E-136	8.51E-07	3.68E-10
Ar [19]	3.40E-10	1.70E-21	1.05E-77	1.62E-134	1.05E-05	1.62E-08
He [21]	2.56E-10	1.41E-22	1.59E-79	4.47E-137	1.59E-07	4.47E-11
Kr [21]	3.68E-10	2.30E-21	2.28E-77	5.67E-134	2.28E-05	5.67E-08
Xe [21]	4.07E-10	3.10E-21	5.64E-77	2.56E-133	5.64E-05	2.56E-07
CO ₂ [20]	4.50E-10	4.00E-21	1.32E-76	1.10E-132	0.000133	1.10E-6

$$B=1.0E-7 \text{ nN-nm nm}^{12} \quad [22]$$

Configuration 1- atomic ring with no pressure

The energy and force values for the atomic ring with no pressure behave in the same manner as the basic model. Because this configuration has no internal pressure, the values of energy and force will be the same as the basic model. The geometry of the atomic ring has no affect on the bonding mechanisms between two atoms. A graphical representation of the energy and force for this configuration is shown in Figures 1 and 2.

Configuration 2- atomic ring with internal pressure

The atomic ring with internal pressure behaves the same as configuration 1 and that of the simplest two atom model. While these two concepts behave in the same manner, the addition of an internal pressure does affect the interaction between atoms. The values of energy and force are affected by the distance the atoms move outward because of the force pushing outward. The equilibrium separation in configuration 2 is greater than configuration 1 due to the addition of internal pressure. This increase in equilibrium separation is the defining term for the configurations with internal pressure.

The comparison of the potential energy in the atomic ring with no pressure to the atomic ring with internal pressure determines that the amount of energy tends to increase when pressure is added. Comparison between the resultant forces of the two atomic ring configurations show that the amount of resultant force capable tends to increase when pressure is added to the atomic ring. These two comparisons indicate that a pressure force causes both the energy and the force to increase as the equilibrium separation increases.

Configuration 3- atomic sphere with no pressure

The atomic sphere configuration behaves like the atomic ring configuration with no pressure. Looking at the geometry of the third configuration it appears that a sphere is capable of maintaining a greater equilibrium separation than a ring. However, because there is no pressure involved in the configuration, the equilibrium separation of a sphere with no internal pressure is capable of the same equilibrium separation as the atomic ring with no internal pressure. Since the equilibrium separation for this third configuration is the same as the configuration 1, it is concluded that the energy and forces are the same as the basic two atom model.

Configuration 4- atomic sphere with internal pressure

The final configuration of this study is an atomic sphere with an internal pressure. This configuration's results can be compared to that of configuration 2. The energy and force values of the atomic sphere with internal pressure are the same as the atomic ring with internal pressure. Comparing the energy and force values of configurations 1 and 3 to the final setup, the values in this final configuration will be greater because of the increase in equilibrium separation due to the addition of an internal pressure.

VI. Comparison with documented surface tension

Surface tension is an effect that causes a liquid to behave like an elastic sheet. It is caused by the attraction between molecules due to the intermolecular forces. On a surface the molecules are pulled inward by the molecules within a liquid. Surface tension is defined as “the force along a line of unit length perpendicular to the surface or work done per unit area” [5].

For surface tension measurement it is often safest to regard the values obtained to be merely a measure of success of the mathematical analysis. It is determined that, with the exception of water and benzene, there is no absolute value of surface tension that has been agreed upon to within one-tenth of 1 % for liquids. This is because of the variation of one part in 1000 in surface tension. However, in most investigations of surface phenomena, it is sufficient to measure relative values or variations instead of actual values [23]. For this reason, current knowledge of surface tension is understood from testing rather than from mathematical modeling.

As one of the fundamental parameters, surface tension is one of the single most accessible experimental parameters that describe the

thermodynamic state [17]. Its importance on the behavior of fluids and fluid mixtures has caused it to be one of the most studied physical properties in the last century. The classic equation for surface tension is given by van der Waals; however, by replacing the classic equation with one used to reproduce thermodynamic singularities at the critical point, Fisk and Widom were able to make predictions of the surface tension at the critical point [18].

For the final purpose of this study, a comparison is made between the current documented experimental data for surface tension and surface tension predicted in this study based on the Lennard-Jones potential.

Within the forces determined by the Lennard-Jones potential equations there is a critical pressure force (P_{cr}). This P_{cr} is important to the ability to calculate the surface tension mathematically. The ability to do this comes from previous knowledge of spheres and surface tension.

Figure 12 is a depiction of the geometry used to determine equations 39 through 46. The relationships between the desired unknowns are shown and developed. The following equations are used to develop a computer program to predict surface tension, see Appendix. The symbols in these equations are illustrated in Figures 12 and 3.

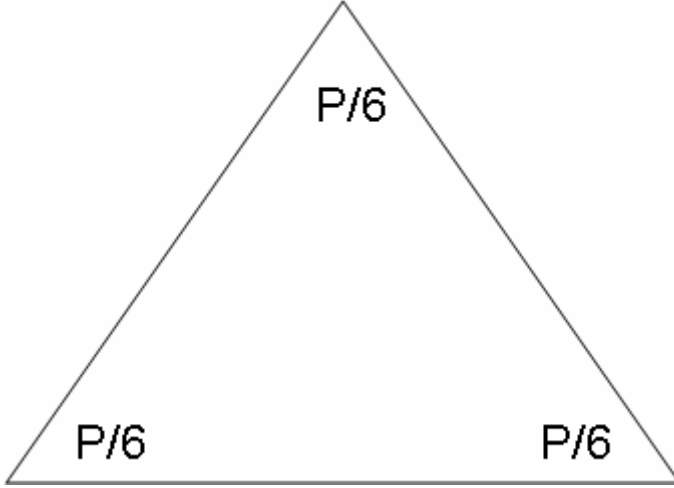


Figure 12: Depiction for pressure determination

$$e = R \left(\frac{r_{\max}}{r_e} - 1 \right) \quad (39)$$

$$F_{\max} = \frac{6A}{r_{\max}^7} - \frac{12B}{r_{\max}^{13}} \quad (40)$$

$$\theta = \frac{r_e}{R} \quad (41)$$

$$P_{cr} = 6F_{\max} \left(\frac{\theta}{2} \right) \quad (42)$$

$$Area = \frac{1}{2} r_{\max} (0.866) \quad (43)$$

$$\frac{P_{cr}}{6Area} = \frac{2\gamma}{r} \quad (44)$$

$$p = \frac{3P_{cr}}{6Area} \quad (45)$$

$$\gamma = \frac{pr}{2} \quad (46)$$

These equations are the essence of the thesis. Equation 46, in particular, mathematically relates surface tension to internal pressure as determined from the Lennard Jones potential. Figure 12 is essential to the model; it is a 1/6th representation of the hexagon configuration seen in Figure 10a. At each corner there are 5 other triangles coming into the point, which leads to the conclusion that at each corner is a pressure of 1/6th the total pressure.

For example the A and B values for mercury are $A=2.79E-5$ nN-nm nm⁶ and $B=1.66E-8$ nN-nm nm¹². Assuming a radius of 1 mm for a bubble and using the above equations it is shown that for mercury the calculated and documented surface tensions match as seen in Table 2.

Table 2: Determination of Surface Tension Hg

Determination of Surface Tension of Mercury						
A =	2.79E-05	nN-nm nm ⁶			gamma =	425mN/m
B =	1.66E-08	nN-nm nm ¹²				
R =	1	mm =	1000000	nm		
Theta =	3.30E-07	Rad				
r _e =	3.30E-01	Nm				
r _{max} =	3.61E-01	Nm				
e=	9.40E-02	mm =	9.40E+04	nm		
F _{max} =	9.69E-02	nN				
P _{cr} =	9.59E-08	nN				
Area =	5.64E-02	Nm ²				
P =	8.4991E-07	nN/nm ² =	0.849909586	Pa		
gamma =	0.424954793	nN/nm (N/m)				
gamma =	424.9547932	mN/m				

Equation 46 is the essential equation for this model; it is shown numerically that surface tension is not a function of the radius.

Tables 3 and 4 are representations of the comparisons between the experimental surface tension and calculated surface tension values. From Table 2, 3, 4, and the tables located in the appendix; the results show that the values between the documented and calculated surface tensions are either close or match in value.

In Table 3 surface tension comparison for the basic elements are found; thus, we are able to examine the Lennard- Jones potential values next to the surface tensions calculated from this data and to the experimental data found in the literature. It is maybe concluded that, for the most part, the calculated values of surface tension match those that have been experimentally determined. However, for those surface tensions that are very close to the experimental values, the error can be found in the values of the Lennard-Jones constants. For the error found in the Lennard- Jones constants A and B, it is assumed that there is a calculation error in how those values for specific elements are found. Since A and B are based on the epsilon and sigma values, this is where the calculation error occurs. For some elements, changing the values of

Table 3: Surface Tension Comparison of basic elements

Element	σ (m)	ϵ (J)	A Lennard Jones constant (nN-nm ⁶)	B Lennard Jones constant (nN-nm ¹²)	Calculated Surface Tension (mN/m)	Experimental Surface tension (□mN/m)
in general	3.16E-10	2.50E-21	1.00E-04	1.00E-07		
Hg	2.9E-10	1.174E-20	2.79E-05	1.66E-08	424.9	425
Ne	2.75E-10	4.92E-22	8.51E-07	3.68E-10	19.8	16
Ar	3.40E-10	1.70E-21	1.05E-05	1.62E-08	44.89	42
Kr	3.68E-10	2.30E-21	2.28E-05	5.67E-08	51.5	52.1
Xe	4.07E-10	3.10E-21	5.64E-05	2.56E-07	57.2	61
He	2.56E-10	1.41E-22	1.59E-07	4.47E-11	6.58	0.12

A and B allows for the matching values of surface tension that currently do not match the experimental values to be obtained.

The model being used in the study is accurate for the basic elements being examined, with the exception of helium. In the case of helium, the experimental value of the surface tension is still disputed by several sources. In recent studies, it has been determined that for liquid helium the results obtained for the value of surface tension has differed by as much as 6% [24]. This knowledge, that the value of surface tension for helium is still disputed, makes it possible for the model in this study to be accurate for the basic element helium. However, when further work on the surface tension of helium is completed, those results will prove if the model is accurate for the basic element helium. If future work shows that the value for surface tension obtained is not equal to what is

predicted by the model, it is assumed that the make-up of helium atoms indicates why the model is not accurate.

In Table 4 comparison of surface tension data is continued for several molecules. The table shows that for the molecules, the values of surface tension do not match with documented values. However, for the molecule carbon tetrachloride, changing the value of the Lennard-Jones constants allows for the documented value of surface tension to be obtained. For the two other molecules found in Table 4, it is concluded that the model being used is only accurate for smaller molecules. In this model, the length between atoms is important. For molecules the length between the atoms is unknown, and because of the varying number of atoms that can be in a molecule, it is unknown how these affect the model. Further work along these lines is needed to develop simulation models for larger molecules.

Table 4: Surface Tension Comparison of Molecules

Element	σ (m)	ϵ (J)	A Lennard Jones	B Lennard Jones	Calculated Surface	Experimental Surface
In general	3.16E-10	2.50E-21	1.00E-04	1.00E-07		
CCl ₄	5.88E-10	4.51E-21	7.46E-04	3.08E-05	39.8	26.43
CO ₂	4.50E-10	4.00E-21	0.000133	1.10E-06	60.6	5
H ₂ O	3.17E-10	1.08E-21	4.34E-6	4.36E-9	32.8	72

VI. Conclusion

This studies purpose is to mathematically determine surface tension. The study is directly prompted by a need to better understand the ability to mathematically determine surface tension. The elements examined for the study were arbitrarily chosen. Using the documented values for constants A and B surface tension was mathematically determined for the elements and molecules. For the basic elements chosen the predicted surface tension agrees with the documented surface tension. The model is also used to predict the surface tension of larger molecules, while the calculated values are in the ball park the numbers don't agree with what is in the literature. Future studies need to be done to account for the larger molecules. However, based on this work it is encouraging that surface tension can be mathematically calculated.

Bibliography

List of References

- [1] Barnes,G.T.,Gentle, I.R., *Interfacial Science*. Oxford University Press.
New York, N.Y., 2005. pp1-9
- [2] Dareing, Don and Thundat,Thomas., *Mechanics of Micro and Nano Systems*. Class Notes. Spring 2006
- [3] <http://hyperphysics.phy-astr.gsu.edu/Hbase/surten.html>
- [4] http://www.ksvinc.com/surface_tension1.htm
- [5] http://en.wikipedia.org/wiki/Surface_tension
- [6] Institute of Nanotechnology. <http://www.nano.org.uk/nano.htm>April 14,
2006.
- [7] Bhushan, Bharat Ed., *Springer Handbook of Nanotechnology*.Springer-Verlag., Berlin, Germany, 2004
- [8] <http://polymer.bu.edu/Wasser/robert/work/node8.html>
- [9] Ashcroft, Neil W.; Mermin, N. David, *Solid State Physics*, Holt, Rinehart and Winston, New York, 1976, p398-401.

- [10] Doane, Lee Peter. Nano Mechanics of Micro Cantilever beam excited
by interactive atomic forces. 2003.
- [11] http://en.wikipedia.org/wiki/Surface_energy
- [12] Kralchevsky, Peter A., Denkov, Nikolai D. *Capillary forces and structuring in layers of colloid particles*. Current Opinion in Colloid & Interface Science 6. 2001. pp383-401.
http://www.colorado.edu/physics/phys7450/phys7450_sp05/colloids/interfacial%20colloids/kralchevsky_2001.pdf
- [13] <http://pubs.acs.org/cgi-bin/abstract.cgi/langd5/2005/21/i24/abs/la0517639.html>
- [14] <http://www.chem.purdue.edu/gchelp/liquids/character.html>
- [15] Langhaar, Henry L. *Energy Methods in Applied Mechanics*. John Wiley & Sons, Inc. New York, NY. 1962.
- [16] <http://www.ctcms.nist.gov/~powell/mrs98/node11.html>
- [17] <http://en.wikipedia.org/wiki/Sphere>
- [18] <http://www.math.unce.edu>

[19] www.diracdelta.co.uk/science/source/l/e/lennard-jones%20potential/source.html. Science and Engineering encyclopedia.

[20] Tabor, David. Gases, liquids, and solids and other states of matter.
3rd

Edition. Cambridge University Press, New York, NY. 1991. pp 30

[21] <http://authors.library.caltech.edu/1157/01/mccjcp95.pdf>

[22] Israelachvili, Jacob. *Intermolecular and Surface Forces* 2nd
Edition. New

York, NY. 1992.

[23] Potoff, Jeffery. Surface tension of the three-dimensional Lennard-Jones fluid from histogram-reweighting Monte Carlo simulations. Journal of Chemical Physics. Vol 223, No 14. April 2000.

[24] <http://funphysics.jpl.nasa.gov/technical/library/sig-events-02/sig021024-science-a.html>

Appendix

Appendix

Tables A.1 through A.9 show the Lennard-Jones constants, radius, angle theta, equilibrium separation (r_e), maximum radius, maximum Force, pressure, critical pressure, and the area being used to calculate the surface tension. For all molecules being modeled the radius (R) is set to be 1 mm.

Table A.1: Determination of Surface Tension CCl_4

Determination of Surface Tension of Carbon Chloride						
A =	7.46E-04	nN-nm nm ⁶			gamma =	26.4mN/m
B =	3.08E-05					
R =	1	mm =	1000000	nm		
Theta =	6.69E-07	rad				
r_e =	6.69E-01	nm				
rmax =	7.32E-01	nm				
e =	9.40E-02	mm =	9.40E+04	nm		
Fmax =	1.84E-02	nN				
Pcr =	3.69E-08	nN				
Area =	2.32E-01	nm ²				
P =	7.96957E-08	nN/nm ² =	0.079695706	Pa		
gamma =	0.039847853	nN/nm (N/m)				
gamma =	39.84785309	mN/m				

Table A.2: Determination of Surface Tension H₂O

Determination of Surface Tension of Water						
A =	4.34E-06	nN-nm nm ⁶			gamma =	72mN/m
B =	4.36E-09					
R =	1	mm =	1000000	nm		
Theta =	3.60E-07	rad				
re =	3.60E-01	nm				
rmax =	3.94E-01	nm				
e =	9.40E-02	mm =	9.40E+04	nm		
Fmax =	8.18E-03	nN				
Pcr =	8.83E-09	nN				
Area =	6.72E-02	nm ²				
P =	6.57559E-08	nN/nm ² =	0.065755946	Pa		
gamma =	0.032877973	nN/nm (N/m)				
gamma =	32.87797279	mN/m				

Table A.3: Determination of Surface Tension Ne

Determination of Surface Tension of Neon						
A =	8.51E-07	nN-nm nm ⁶			gamma =	16mN/m
B =	3.68E-10					
R =	1	mm =	1000000	nm		
Theta =	3.13E-07	rad				
re =	3.13E-01	nm				
rmax =	3.42E-01	nm				
e =	9.40E-02	mm =	9.40E+04	nm		
Fmax =	4.29E-03	nN				
P cr =	4.02E-09	nN				
Area =	5.07E-02	nm ²				
P =	3.96715E-08	nN/nm ² =	0.039671493	Pa		
gamma =	0.019835747	nN/nm (N/m)				
gamma =	19.83574672	mN/m				

Table A.4: Determination of Surface Tension Ar

Determination of Surface Tension of Argon						
A =	1.05E-05	nN-nm nm ⁶			gamma =	42mN/m
B =	1.62E-08					
R =	1	mm =	1000000	nm		
Theta =	3.87E-07	rad				
re =	3.87E-01	nm				
rmax =	4.23E-01	nm				
e =	9.40E-02	mm =	9.40E+04	nm		
Fmax =	1.20E-02	nN				
P cr =	1.39E-08	nN				
Area =	7.75E-02	nm ²				
P =	8.97835E-08	nN/nm ² =	0.089783491	Pa		
gamma =	0.044891745	nN/nm (N/m)				
gamma =	44.89174533	mN/m				

Table A.5: Determination of Surface Tension He

Determination of Surface Tension of Helium						
A =	1.59E-07	nN-nm nm ⁶			gamma =	0.12mN/m
B =	4.47E-11					
R =	1	mm =	1000000	nm		
Theta =	2.91E-07	rad				
re =	2.91E-01	nm				
rmax =	3.19E-01	nm				
e =	9.40E-02	mm =	9.40E+04	nm		
Fmax =	1.32E-03	nN				
P cr =	1.16E-09	nN				
Area =	4.39E-02	nm ²				
p =	1.3161E-08	nN/nm ² =	0.013161016	Pa		
gamma =	0.006580508	nN/nm (N/m)				
gamma =	6.580508173	mN/m				

Table A.6: Determination of Surface Tension Kr

Determination of Surface Tension of Krypton						
A =	2.28E-05	nN-nm nm ⁶			gamma =	52.1mN/m
B =	5.67E-08					
R =	1	mm =	1000000	nm		
Theta =	4.19E-07	rad				
re =	4.19E-01	nm				
rmax =	4.58E-01	nm				
e =	9.40E-02	mm =	9.40E+04	nm		
Fmax =	1.49E-02	nN				
P cr =	1.87E-08	nN				
Area =	9.09E-02	nm ²				
p =	1.0316E-07	nN/nm ² =	0.103160299	Pa		
gamma =	0.051580149	nN/nm (N/m)				
gamma =	51.58014944	mN/m				

Table A.7: Determination of Surface Tension Xe

Determination of Surface Tension of Xenon						
A =	5.64E-05	nN-nm nm ⁶			gamma =	61mN/m
B =	2.56E-07					
R =	1	mm =	1000000	nm		
Theta =	4.63E-07	rad				
re =	4.63E-01	nm				
rmax =	5.06E-01	nm				
e =	9.40E-02	mm =	9.40E+04	nm		
Fmax =	1.83E-02	nN				
P cr =	2.54E-08	nN				
Area =	1.11E-01	nm ²				
p =	1.14404E-07	nN/nm ² =	0.11440386	Pa		
gamma =	0.05720193	nN/nm (N/m)				
gamma =	57.20193024	mN/m				

Table A.8: Determination of Surface Tension CO₂

Determination of Surface Tension of Carbon Dioxide					
A =	1.33E-04	nN-nm nm ⁶			gamma = 5mN/m
B =	1.10E-06				
R =	1	mm =	1000000	nm	
Theta =	5.12E-07	rad			
re =	5.12E-01	nm			
rmax =	5.60E-01	nm			
e =	9.40E-02	mm =	9.40E+04	nm	
Fmax =	2.14E-02	nN			
Pcr =	3.29E-08	nN			
Area =	1.36E-01	nm ²			
p =	1.2122E-07	nN/nm ² =	0.121219829	Pa	
gamma =	0.060609915	nN/nm (N/m)			
gamma =	60.6099146	mN/m			

Vita

Allison Dawn Lewis was born and raised in Knoxville, TN. She attended to Halls Elementary, Middle and graduated from Halls High School in 2001. After high school, she attended the University of Tennessee, Knoxville where she received her Bachelor of Science in Biomedical Engineering with a minor in Aerospace Engineering. Allison received her Master of Science in Biomedical Engineering from the University of Tennessee in Knoxville in 2007.